



Macroscopic cross section generation with WIMS-ANL for a PWR

^aW. Coloma, P. A. L. Reis, C. A. M. da Silva, C. Pereira

^a Departamento de Eng. Nuclear – Universidade Federal de Minas Gerais (UFMG), PCA1—Anexo Engenharia, Av.
Antonio Carlos, 6627 Pampulha 31270-901, Belo Horizonte, MG, Brazil, wilmer.fcfn.fis@gmail.com

ABSTRACT

Based on the BEAVRS Benchmark (Benchmark for Evaluation And Validation of Reactor Simulations) which contains reference specifications for operational data and measurements for a pressurized water reactor (PWR), it presents a model for obtaining macroscopic cross sections for the different fuels assemblies of BEAVRS using the WIMS-ANL. The microscopic cross section data library used was ENDF/B-VI. For the cross-section calculation method, the multicellular model approach was considered, and the results were compared with other reference works. This methodology aims to validate the model of calculation of the cross sections, and thus, evaluate whether such methodology generates valid results. Also, in this work, the macroscopic cross-sections generated by WIMS were used to simulate the reactor core of a typical PWR in PARCS. All calculations were made for the reactor's Hot Zero Power status and the first cycle of operation.

Keywords: Macroscopic cross sections, BEAVRS, PWR.



1. INTRODUCTION

Simulations of the reactor core are essential for the economical and safe operation of a nuclear plant. Currently, several different simulation tools are available and nuclear engineers perform calculations to predict the state of the reactor's core. This work is an example of computational tools applied to perform pressurized water reactor (PWR) simulations. Currently, the complete analysis of the core of a nuclear reactor is still based on the traditional two-step calculation scheme, which has been the standard approach for reactor analysis. These steps consist of: (1) spatial homogenization and condensation of energy groups using cell code, and (2) calculation of the complete core in 3D using few group constants, generated in the previous step. Sanchez's work [1] provides a good review of modern homogenization techniques.

The main objective of this work was to generate the macroscopic cross sections, to carry out tests and evaluations of the methodology in two stages WIMS-PARCS [2], [3], with a benchmark problem, based on real data. In addition, the development and verification of the mathematical model of the nuclear reactor PWR was also a goal.

In this work, the benchmark known as BEAVRS [4] was used, which comes from Evaluation And Validation of Reactor Simulations. BEAVRS is a full-scale PWR-based benchmark, containing 193 fuel assemblies (FA). These FAs consist of 3 different types of enrichment, that is, 1.6, 2.4 and 3.1 weight percent ^{235}U . These 3 different enrichment-based FAs may contain different arrangements of burnable absorbers (BAs). Each FA is a 17×17 array of fuel pins. A total of 8 grid spacers (6 intermediates, one above and one below) are present in each FA.

BEAVRS was published in 2013 by the Computational Reactor Physics Group of the Massachusetts Institute of Technology (MIT) and has been updated several times. Its purpose is to allow the comparison of various computer codes of reactor physics applied to full-core calculations with real data. The reference specification contains a detailed description of an unknown (real) nuclear power plant for a 4-circuit Westinghouse reactor located in the USA. The documentation contains details of the power measurements and operating conditions of the reactor for the first and second fuel cycles. More details on BEAVRS can be found in the original reference document [4]. Several research reports on BEAVRS solutions have been published for a wide variety of simulation

methodologies [5]–[14]. The model developed in this work was compared with benchmark data available for the first fuel cycle presented in the publications [4], [5], [8], [14], [15]

The methodology consists of two stages. In the first step, the macroscopic cross sections of the fuel elements with the code WIM-ANL 5.08 will be calculated. The microscopic cross section data library used was ENDF/B-VI. In the second stage, the cross sections obtained will be used to simulate the entire reactor with the PARCS 2.4 code; these simulations are made for the reactor's Hot Zero Power (HZP) state and for the first cycle of operation.

2. METHODOLOGY

2.1. Obtaining macroscopic cross sections

The WIMS code family allows the calculation of neutron flux distributions, k -inf and k -eff values in a variety of reactors. Typically, the WIMS-ANL 5.08 reactor physics code has been used as a tool for lattice calculations to generate homogenized reactor physics parameters for a whole core (i.e. traditional two-step analysis)

In this work, the MULTICELL method will be used. The MULTICELL approach is only an alternative but offers an additional possibility that any of the cells in Fig. 1a can also be a group of pin cells by themselves. Any of these cells, which for some reasons are considered different from the others, can be calculated independently. The calculation is performed separately for each cell type, but the usual boundary condition is replaced by "intercellular boundaries" expressed in terms of the probabilities that a neutron will leave one cell type and enter another. This is expressed schematically in Fig. 1b, where the cells were separated for the calculations and their interconnections must be provided from outside. Fig. 1c illustrates that cell types can differ not only in composition but also in dimensions [4].

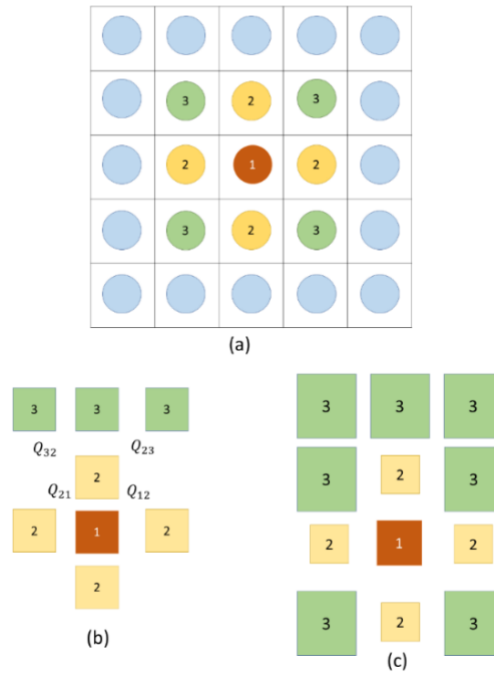


Figure 1: Schematic interpretation of the MULTICELL approach (a) Macrocell to be calculated with the cell types chosen (b) The calculation of the spectrum of 69 groups is carried out separately for each type, (c) The cells may differ in composition and geometry.

Two basic probabilities are presented:

$P_{iA,jB}$: the probability that a neutron born in region i of cell A will have its first collision in region j of cell B, and

Q_{AB} : the probability that a neutron leaving the boundary of cell A will have a collision in cell B.

For these probabilities, it can write:

$$P_{iA,jB} = \delta_{AB}p_{ij} + p_{ib}^A \cdot Q_{AB} \cdot \frac{p_{bj}^B}{(1 - p_{bb}^B)} \quad (1)$$

where

p_{ij} : the probability that a neutron born in region i will have its first collision in region j .

p_{ib}^A : the probability that a neutron born in region i of cell A will reach the limit of the cell without collision,

$$p_{bb}^B = 1 - \sum_{j=1}^J p_{bj}$$

p_{bb}^B : the probability that a neutron will appear at the cell boundary to have its first collision in region j .

To determine Q_{AB} , it can assume that $Q_{AB} = S_{AB}$ is the probability that a neutron leaves the surface of cell A, and enters the surface of cell B. So S_{AB} is purely geometric, that is, its elements are fractions of surfaces A and B, that is, it is a fraction of cell surface A contiguous to B. More details about the multicell model can be found in [16].

For the simulation of the fuel assemblies, different macrocells were considered, which are composed of cells. The macrocell selection criterion consisted in distinguishing whether a group of cells of equal size and composition share the same interaction probabilities with the neighboring cells, if it is equal in size and composition. Therefore, each group of cells of the same macrocells are equal. It should be noted that the macrocells are not necessarily the same as others, that is, each one will have a different geometry and composition. Figure 2 shows the choice of macrocells for all FAs of the first cycle. Cells of the same color represent a type of macrocell.

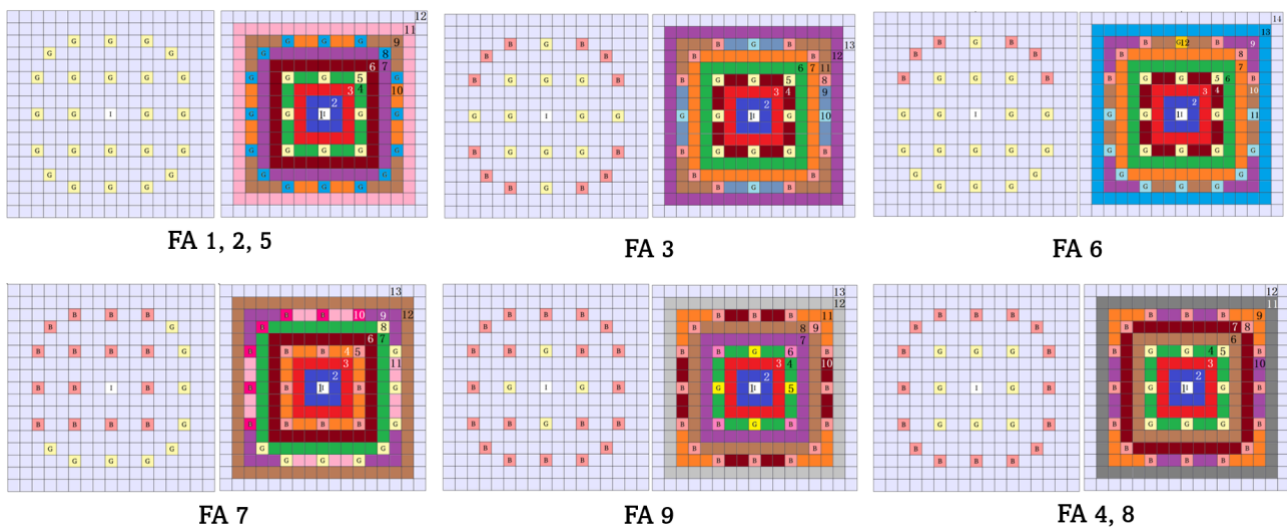


Figure 2: shows the FAs and the choice of the corresponding macro cells for each FA. Each macro cell is identified with a different color.

It can be seen that FA 1, 2 and 5 share the same choice of macro cells, this is because these FAs are the same in geometry, one is different from another only in uranium enrichment. The same happens with FA 4 and 8.

There are 4 different cells in all FAs. These cells are presented in figure 3. Figure 3a shows the cell that contains the fuel rod, this cell, depending on the type of FA, will have different enrichment.

Figure 3 b shows the cell that contains the guide tube, this cell will be the same in all FAs. Figure 4c shows the cell that contains the burnable poison, this cell will be the same for all FAs. Figure 4d shows the cell that contains the instrumentation tube, this cell will be the same in all FAs. And figure 4 e shows the cell that continues the control rod.

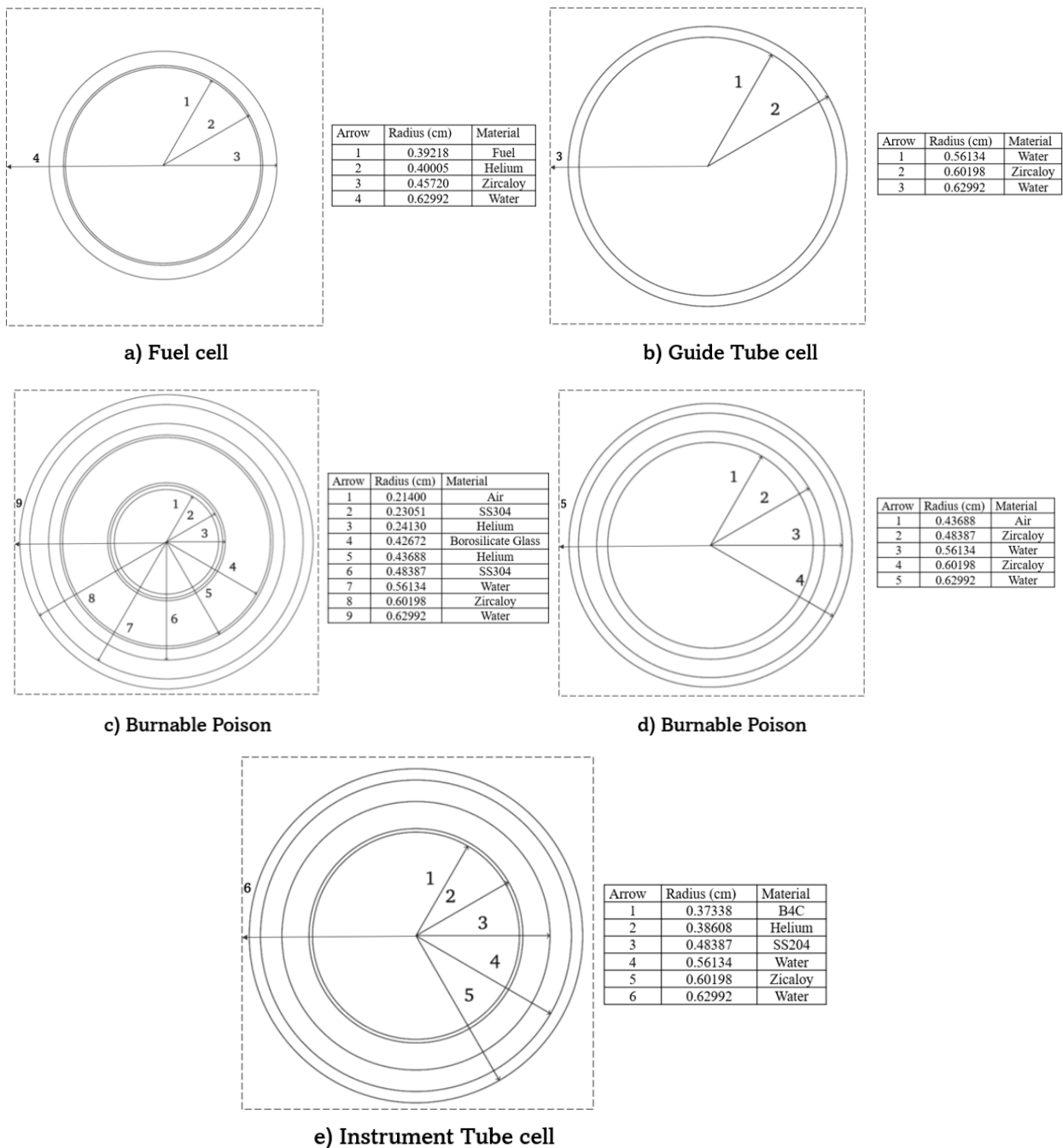


Figure 3: Cells that make up the fuel assemblies.

Information on the composition and density of materials are detailed in BEAVRS [4].

2.2. Reactor core model with PARCS

The model of the reactor core with PARCS, will have the same radial nodalization as the standard load of the reactor core (BEAVRS core), a node for a FA and a total of 257 nodes. The axial nodalization consists of 50 axial levels of the active core of equal length and two reflecting nodes, upper and lower (See Fig. 4).

Another model has been added for the axial and radial reflector. The suggestions made in the WIMS user manual for simulating reflectors were used [2]. In order to simulate the radial reflector, the FA in grey (see Fig. 4a), was applied as an additional square region, having the same size as the other FA (Fig. 4b). And it is filled with 2 regions: water and steel (Stainless Steel) [4]. In addition, for the sake of simplicity and to reduce computational effort, the spacer grid models were not considered. e

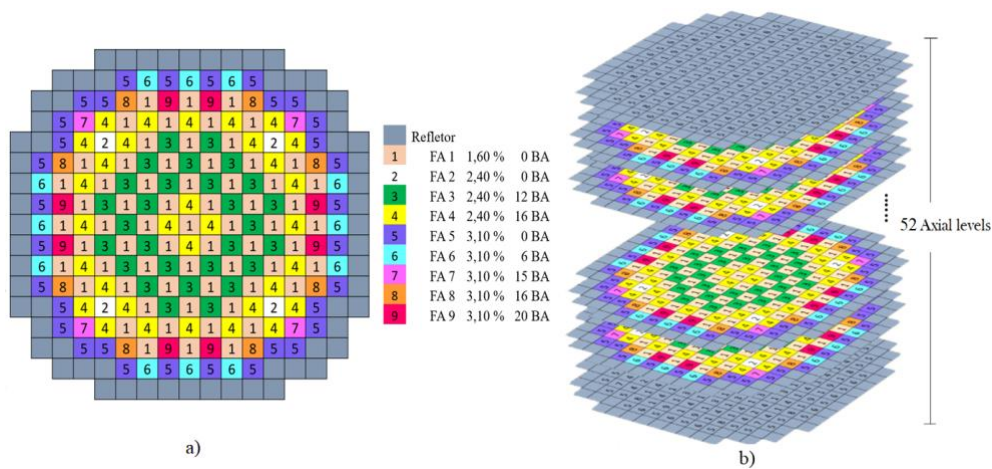


Figure 4: a) Radial profile modelled on PARCS of BEAVR, b) Axial profile of the core modelled on PARCS.

To have a complete model, it is necessary to obtain the cross sections of the reflector. Due to the need to include the reflector, it was adopted the methodology suggested in the user manual WIMS-ANL, which consists of homogenizing the fuel elements neighbouring the reflector (See Fig. 5). This homogenization allows the WIMS to use the spectrum of neutrons from the fuel assembly to obtain only the homogenized macroscopic cross sections of the reflector.

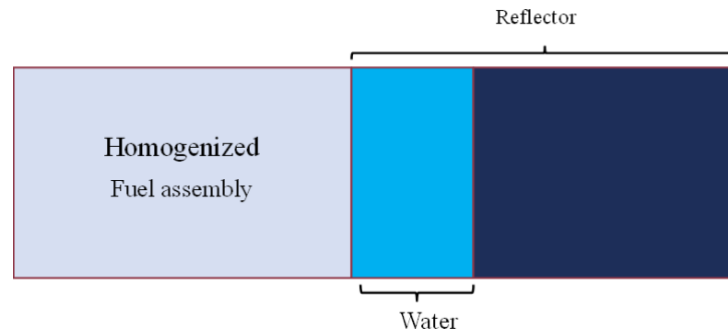


Figure 5: Schematic model to obtain the macroscopic cross sections of the reflector.

The first step to validate the methodology will be to simulate the core under Hot Zero Power (HZIP) conditions. The parameters for the simulation under these conditions are shown in Table 1. More details about the HTZ conditions can be found in the benchmark [4].

Table 1: Parameters used in WIMS-ANL inputs for HZIP.

Fuel temperature	566 K
Coolant temperature	566 K
Number of groups	48
Boron concentration	975 ppm

The number of groups for the simulation is 48 because the values obtained from k_{eff} will be compared with the works by Ryu and Park [11], [5] and in these works, the number of groups used is 48.

For the burn-up conditions, the MULTICELL model was also used, no major changes were made in the structure of the inputs in the HZIP state, only the card that activates the fuel burn-up was added. The parameters used are shown in Table 2. Both the HZIP (Table 1) and the HFP (Hot Full Power) (Table 2) were considered an average temperature for both the coolant and the fuel in all the different fuel assemblies, according to the benchmark.

In the reactor operating condition (HFP and during the fuel burn-up), as already mentioned, this work follows the two-step neutron simulation methodology. The first step is to obtain the cross sections for each FAs. The output of the WIMS-ANL offers the possibility to obtain the cross sections during each burning period (range of operating days). In this work, 23 time intervals were used, in each of them, the reactor is at a certain operating power, which are detailed in BEAVRS [2]. The second step consists of using the cross sections as input to simulate the core with the PARCS 2.4 code.

Table 2: Parameters at HFP (Hot Full Power) and used for fuel burn-up.

Fuel temperature	900 K
Coolant temperature	566 K
Initial boron concentration	975 ppm
Days of Operation (Cycle 1)	575 days

Table 3 shows the information corresponding to the intervals of days and the corresponding operating powers during the first burning cycle.

Table 3: Information on the days of operation and performance for the first cycle.

Days	Power MWt	Power %
0	24.07	0.706
7	119.61	3.507
18	692.69	20.31
54	1105.96	32.42
62	1660.93	48.69
66	1668.06	48.9
81	2525.37	74.04
82	2495.8	73.17
88	3051.7	89.47
92	3365.7	98.67
161	2205.55	64.66
169	3403.53	99.78
187	3410.19	99.98
218	3198.76	93.78
251	3397.52	99.6
323	2171.18	63.65
339	3400.67	99.7
368	3387.21	99.3
403	3406.24	99.86
434	3394.29	99.51
468	3407.78	99.91
504	3403.71	99.79
551	2881.59	84.48
573	2382.84	69.86

3. RESULTS AND DISCUSSION

The first step consisted of obtaining the macroscopic cross sections, to later use them in the simulation of the complete reactor with the PARCS code. Due to a large amount of data from the cross sections, in this section, it will present only the k-eff values for Hot Zero Power state. In this first stage, the configuration of cycle 1 [4] was simulated, which consists of FAs with different enrichments and different numbers of BAs in each FA, as shown in Fig. 4a. All these values are shown in table 4.

Table 4: k-eff results for the different FA, obtained with the codes WIMS-ANL, nTRACER and McCARD [5].

FA	w/o U235	BA	WIMS-ANL	nTRACER	McCARD	Dev.Std
FA 1	1.6	0	0.989864	0.99340	0.99483	0.0025563
FA 2	2.4	0	1.130619	1.13696	1.13751	0.0038296
FA 3	2.4	12	1.006204	1.01318	1.01432	0.0043938
FA 4	2.4	16	0.972506	0.97454	0.97597	0.0017407
FA 5	3.1	0	1.211479	1.21971	1.21971	0.0047521
FA 6	3.1	6	1.127674	1.16273	1.16313	0.0203560
FA 7	3.1	15	1.065516	1.07835	1.07895	0.0075888
FA 8	3.1	16	1.059016	1.06340	1.06416	0.0027766
FA 9	3.1	20	1.021857	1.02769	1.02886	0.0037513

The PARCS core model has the same radial nodalization as the reactor core loading pattern. Figure 4 shows the axial distribution of the detector measurements (orange circles) provided with the BEAVRS specification (Hot Zero Power condition). It also shows the values that were calculated with PARCS (blue circle). It can seem that these points are quite like each other, with a maximum relative error of 14.29% over the first point of the axial length (Figure 6).

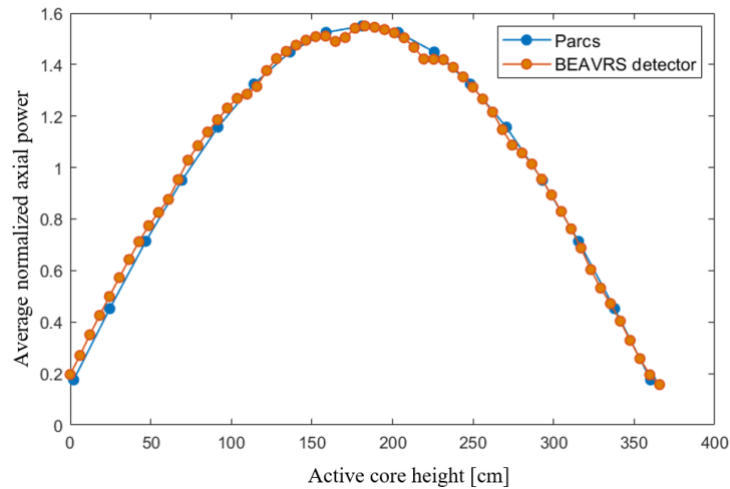


Figure 6: Distribution of axial power of BEAVRS (orange dots). Axial power distribution calculated by PARCS (blue dots).

Figure 7 shows the boron concentration history throughout the burnup for the first cycle of reactor operation. And the same figure shows the data obtained with PARCS-WIMS and the data measured by the detector is also presented.

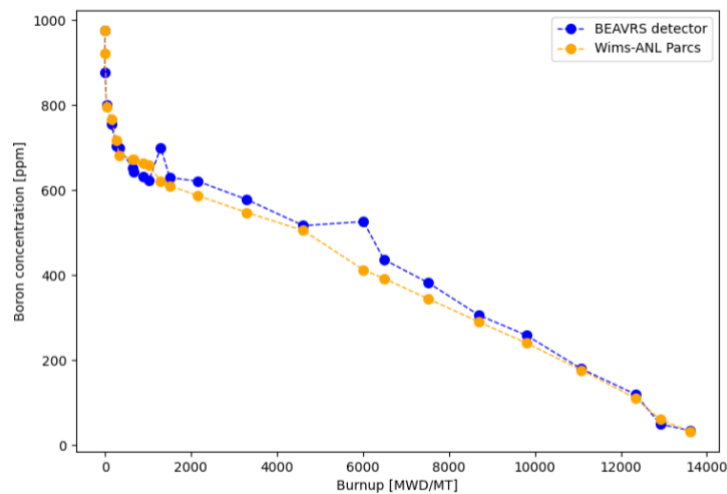


Figure 7: Comparison of the boron measurements [2] performed during Cycle 1 with WIMS-PARCS calculations.

The comparison of the PARCS results with the BEAVRS boron concentration measurements taken at the time of the detector measurements is shown in figure 7. The most significant difference was observed for the 6012 MWD/MT operating point with a relative error of 21.5%.

4. CONCLUSION

The data specified in the BEAVRS were used to simulate the reactor core, which consisted of two stages. The first step consisted of calculating macroscopic cross sections, these data were obtained with the WIMS-ANL code. With the model used in WIMS-ANL, the k-eff of each fuel assemblies were calculated; the maximum standard deviation of the results was 0.02. The second step is to use the cross sections in the PARCS input file, with which the axial power distribution was obtained. The boron concentration was also obtained throughout the burnup during the first cycle of operation.

ACKNOWLEDGMENT

The authors are grateful to the Coordenação de Aperfeiçoamento de Pessoal de Nível Superior (CAPES), the Fundação de Amparo à Pesquisa do Estado de Minas Gerais (FAPEMIG), and the Conselho Nacional de Desenvolvimento Científico e Tecnológico (CNPq) for the support.

REFERENCES

- [1] R. SANCHEZ, Assembly homogenization techniques for core calculations, **Progress in Nuclear Energy**. 2009, doi: 10.1016/j.pnucene.2008.01.009.
- [2] J. R. DEEN, W. L. WOODRUFF, I. C. COSTESCU, AND L. S. LEOPANDO, WIMS-ANL USER MANUAL REV. 6, **ARGONNE**, ILLINOIS, 2004.
- [3] T. K. T. DOWNAR, Y. XU, PARCS v2.7 USER MANUAL U.S. NRC Core Neutronics Simulator, **W. Lafayette**, Indiana, 2006.
- [4] N. HORELIK, B. HERMAN, B. FORGET, AND K. SMITH, Benchmark for evaluation and validation of reactor simulations (BEAVRS), in **International Conference on Mathematics and Computational Methods Applied to Nuclear Science and Engineering, M and C 2013**, v. 4, p. 2986–2999, 2013.
- [5] H. J. PARK, S. J. KIM, H. KWON, AND J. Y. CHO, BEAVRS benchmark analyses by DeCART stand-alone calculations and comparison with DeCART/MATRA multi-physics coupling calculations, **Nucl. Eng. Technol.**, 2020, doi: 10.1016/j.net.2020.02.015.
- [6] Z. WANG, B. WU, L. HAO, H. LIU, AND J. SONG, Validation of SuperMC with BEAVRS

- benchmark at hot zero power condition, **Ann. Nucl. Energy**, vol. 111, p. 709–714, 2018, doi: 10.1016/j.anucene.2017.09.045.
- [7] M. A. ELSAWI AND A. S. B. HRAIZ, Benchmarking of the WIMS9/PARCS/TRACE code system for neutronic calculations of the Westinghouse AP1000TM reactor, **Nucl. Eng. Des.**, 2015, doi: 10.1016/j.nucengdes.2015.08.008.
- [8] D. LI *et al.*, JMCT Monte Carlo Simulation Analysis of BEAVRS and SG-III Shielding, **CRS-13 & RPSD**, 2017, doi: 10.1051/epjconf/201715306017.
- [9] J. YU, H. LEE, M. LEMAIRE, H. KIM, P. ZHANG, AND D. LEE, Fuel performance analysis of BEAVRS benchmark Cycle 1 depletion with MCS/FRAPCON coupled system, **Ann. Nucl. Energy**, 2020, doi: 10.1016/j.anucene.2019.107192.
- [10] C. LIN, J. I. YANG, K. J. LIN, AND Z. DE WANG, Pressurized water reactor loading pattern design using the simple tabu search, **Nucl. Sci. Eng.**, v. 129, p. 61–71, 1998. doi: 10.13182/NSE98-A1963.
- [11] M. RYU, Y. S. JUNG, H. H. CHO, AND H. G. JOO, Solution of the BEAVRS benchmark using the nTRACER direct whole core calculation code, **Nucl. Sci. Technol.**, 2015. doi: 10.1080/00223131.2015.1038664.
- [12] B. COLLINS, A. GODFREY, S. Stimpson, and S. Palmtag, Simulation of the BEAVRS benchmark using VERA, **Ann. Nucl. Energy**, v. 145, 2020. doi: 10.1016/J.ANUCENE.2020.107602.
- [13] P. CIVITA, P. FORNACIARI, AND T. MAZZANTI, Optimal Operational Strategy in Nuclear Fuel Management, **Nucl. Technol.**, v. 14, no. 2, p. 116–122, 1972. doi: 10.13182/nt72-a31126.
- [14] Z. LI, H. WU, L. CAO, C. TIAN, and D. CHEN, On-line monitoring analysis of BEAVRS benchmark using NECP-ONION, Physor, 2016.
- [15] P. DARNOWSKI AND M. PAWLUCZYK, Analysis of the BEAVRS PWR benchmark using SCALE and PARCS, **Nukleonika**, 2019.
- [16] A. GANDINI, J. J. SCHMIDT, AND S. GANESAN, **Nuclear Reactors-physics, Design And Safety - Proceedings Of The Workshop**. World Scientific Publishing Company, 1995.